

Cytoplasmic Localization of PCV1-VP3 is a CRM1-Independent Function

A Major Qualifying Project Submitted to the Faculty of
WORCESTER POLYTECHNIC INSTITUTE

In partial fulfillment of the requirement for the
Degree of Bachelor of Science

By

Paul Burrowes

Biochemistry

Christine Carbone

Biochemistry

April 25, 2017

Approved:

Dr. Destin Heilman

Advisor

Department of Chemistry & Biochemistry, WPI

Abstract

Members of the *Circoviridae* family, such as PCV1-VP3, encode viral proteins that are capable of selectively inducing apoptosis in transformed cells via a p53-independent mechanism while leaving healthy cells intact. The mechanism by which PCV1-VP3 can "sense" cancer from within the cell and trigger apoptosis may prove to be a viable approach to developing a new form of cancer therapy such as a small molecule drug. In this project, subcellular localization and protein-protein interactions of PCV1-VP3 have been examined in order to more thoroughly characterize the functions that contribute to its cancer-killing activity. In a departure from past groups' mutational approach to characterizing nucleocytoplasmic shuttling of PCV1-VP3, an inhibitor-based assay was developed to test the proteins of interest for CRM1-dependent nuclear export activity. Experimental results revealed that in contrast to the well-characterized nuclear export of Apoptin, PCV1-VP3 does not undergo nuclear export via the CRM1 pathway. In addition, two subdomains of PCV1-VP3, the Core and Tail regions, were found to exhibit differential subcellular localization patterns and appear to contribute unique functions to PCV1-VP3 beyond the Tail's apoptotic activity.

Contents

Abstract	2
Table of Figures	4
Acknowledgements.....	5
Introduction	6
Methodology	13
Transformation of JM109 Competent <i>E. coli</i>	13
Medium Scale Plasmid Purification	13
Cell Culture Maintenance.....	14
Transient Transfections.....	14
Inhibition of the CRM1 Pathway via N-ethylmaleimide.....	15
Cell Fixation	15
Cell Synchronization	16
Time-Course Localization Assay	16
FLAG Immunoprecipitation.....	16
SDS-PAGE	17
Western Blots	17
Results	18
PCV1-VP3 Exhibits CRM1-Independent Subcellular Localization.....	20
Time Course Assay of PCV1-VP3 Subcellular Localization	21
Western Blotting of FLAG and cdc27	21
Discussion	22
Figures & Tables	25
References.....	30

Table of Figures

Figure 1. Protein feature map of proteins used for transfection experiments.	25
Figure 2. Workflow for NEM CRM1 inhibition assay.	26
Figure 3. (A.) N-ethylmaleimide Assay Confocal imaging.	27
Figure 4. Time Course Imaging of PCV1-VP3 wild type; aphidicolin arrest protocol.	28
Figure 5. Western Blotting for FLAG and cdc27.	29

Acknowledgements

First and foremost, we would like to acknowledge our advisor, Destin Heilman, not only for his guidance throughout this project but also for his continued interest and efforts in shaping our undergraduate research experience and our scientific careers. Secondly, we acknowledge Vicki Huntress for providing us with access to the confocal microscope and for training us to use the hardware to collect our fundamental data. We would also like to extend a special thanks to Natalie Farny and Jill Rulfs for engaging us in scientific discussion and for providing us with lab resources to develop and optimize our experimental techniques.

Introduction

Cancer is a devastating disease that affects millions of people. The American Cancer Society estimates that over the course of 2016, over 1.6 million new cases of cancer and approximately 600,000 cancer related deaths will occur in the United States [1]. On a global scale, approximately 19.8 million new cases of cancer will occur each year, and approximately 40% of the population will develop cancer at some point in their lifetime due to a multitude of environmental and genetic factors [2, 3]. These factors lead to mutations in genes—such as proto-oncogenes, tumor suppressor genes, or genes involved in DNA repair—which result in unregulated cell proliferation. If unchecked, the unregulated growth will lead to the development of a tumor. Due to the excessive growth rates, the cancerous cells require a significant amount of metabolic activity primarily in the form of aerobic glycolysis [4]. As the tumor grows, it redirects both cellular and metabolic resources away from the healthy cells which results in deterioration of the affected organ system. Radiation and chemotherapy are the current standard treatment; however, these treatments are harmful to all cells as they are not cancer cell-specific and do not prove effective against all cancer types.

Chemotherapeutic approaches to cancer treatment include a host of DNA-damaging agents that are administered to patients with the goal of destroying cancerous cells. Unfortunately, the DNA damage caused by these compounds lacks specificity for cancer cells, and can result in damage to healthy tissues including bone marrow. As a result, the use of DNA-damaging agents such as chemotherapeutics can increase risk of leukemia if bone marrow is affected. Cisplatin, Carboplatin, and Oxaliplatin are DNA alkylating agents that bind to nitrogen in DNA bases and cause widespread DNA damage [5]. As cells advance through the cell cycle, a network of sensory pathways and regulatory mechanisms serve to detect and respond to DNA damage before a cell divides. If widespread damage is detected, the cell will enter an arrest and will be unable to divide until DNA

damage repair has been completed. Under normal conditions, this response ensures that DNA lesions are repaired accurately (or functionally) and that daughter cells receive full and functional genomes. If a situation arises in which a cell cannot repair DNA damage and recover from the arrest, the cell will be committed to programmed cell death, otherwise known as apoptosis [8]. The apoptotic response ensures that widespread mutations are not passed on to daughter cells in eukaryotic organisms. In the case of chemotherapy with alkylating agents, the severity of DNA damage often prevents repair from completing in rapidly dividing cancer cells and apoptosis is activated as a result [5]. As stated previously, this mechanism of cancer therapy lacks specificity for cancer cells and can damage healthy tissues. Furthermore, cancers can mutate and develop resistance to this treatment method through a number of means. The rates of drug uptake and efflux can be altered by mutation, which ultimately results in kinetically lower rates of DNA damage to favorably mutated cancer cells [5]. DNA repair enzymes may be mutated in ways that improve DNA repair capacity, or the cancer may mutate and increase DNA damage tolerance such that repair and arrest occur at lower rates [5]. A third possibility by which cancers may evade death due to DNA-damaging agents is through mutations in proteins involved in triggering apoptosis pathways [5]. This ultimately results in a failure of the genome's "fail-safe" mechanism, and the cancer cells will continue to proliferate despite widespread DNA damage.

Under typical conditions for a eukaryotic cell, uncontrolled growth is prevented by an array of signaling pathways and checkpoints throughout the cell cycle. Immediately after division, a nascent cell enters G1 phase during which the cell grows in preparation for DNA synthesis. A cell tracked for quiescence will enter G0 phase while cells that are intended to continue dividing will progress through G1. The rate of progression through cell cycle phases is partially regulated by the anaphase promoting complex, or APC. The APC is an E3 ubiquitin ligase that regulates cellular processes by targeting proteins for degradation via polyubiquitination. Typical substrate proteins for the APC are

catalytic enzymes or activating effector molecules such as cyclins [6]. Cyclins are a group of cell cycle regulators that are produced and targeted for degradation at specific points throughout the cell cycle via polyubiquitination of their PEST sequence [7]. These timed degradations of specific cyclins serve to regulate cell-cycle dependent pathways and to signal when conditions are appropriate for the cell to progress to the next phase of the cell cycle. During G1, the APC binds cdh1 via APC subunit 3 (also known as cdc27); this complex (APC/cdh1) prevents the cell from progressing into other cell cycle phases until the cell has grown sufficiently to support cellular division. This process is regulated through polyubiquitination and subsequent degradation of cyclin A, cyclin B, and cell division cycle protein 20 (cdc20) [6]. When the cell is adequately prepared for division, APC/cdh1 is inactivated which allows the cell to progress into S phase—the phase in which DNA is synthesized. After DNA synthesis is completed, the cell can progress into a second period of growth known as G2. During G2, there are several cell cycle “checkpoints” to ensure retained fidelity of DNA after replication. DNA repair mechanisms can trigger a cell cycle arrest via an interaction mediated by the p53 tumor suppressor protein when DNA damage reaches a dangerous level. The G2 arrest provides repair machinery with more time to fix errors before the cell commits to division. If the DNA damage is determined to be irreparable, a pathway mediated by the p53 protein will induce apoptosis [8]. A cell that clears the cell cycle checkpoints will be able to progress into metaphase (M phase) where chromosomal alignment and division between the two daughter cells occurs. Another component of the APC, cdc20, partially triggers this process by complexing with the available APC via cdc27 to form APC/cdc20. This complex initiates polyubiquitination and subsequent degradation of securin which allows for separation of the chromosomes [9]. After complete segregation of sister chromatids by the mitotic spindle, two nuclei form, the plasma membrane is “pinched” to divide the two nuclei (cytokinesis), and two new cells begin the cell cycle again. The interplay between protein synthesis, degradation, and DNA damage sensitivity serves to protect genomic integrity and prevent errant growth; however,

cancers are characterized by widespread mutations to regulatory machinery and exhibit rapid cell cycle progression at the expense of genomic stability.

In roughly 50% of all cancer cases, loss-of-function mutations can be found in a regulatory protein known as p53 that bridges cellular pathways for DNA damage sensing, cell cycle arrest, and apoptosis. Under normal conditions in a cell, p53 protein is regularly expressed and rapidly ubiquitinated by Mdm2 and degraded [10]. DNA damage causes a stress response in cells that activates stress-induced kinases such as ATM, ATR, Chk1 and Chk2 [11]. When active, they post-translationally modify numerous other proteins in the cell by phosphorylating serine and tyrosine residues. Both p53 and Mdm2 are substrates for stress-induced kinases; when phosphorylated, their interaction is disrupted and p53 remains stabilized in the cell. Accumulation of stabilized p53 serves as the link between the DNA-damage stress response and cell cycle regulation machinery. Stabilized p53 is methylated by Set9 (a.k.a. SETD7) and binds DNA at promoter regions of critical genes for cell cycle regulation [12]. Of the host of genes that are transcriptionally upregulated by p53, p21 (a cyclin-dependent kinase inhibitor) causes a cell cycle arrest and prevents cell cycle progression until DNA damage is resolved [13]. If the arrest is not released, cells will either commit to senescence (via p21) or to apoptosis (via p53). Apoptosis serves as a eukaryotic “fail-safe”, and will also activate if the cell is unable to engage senescence through p21. Because of p53’s role in bridging stress responses to cell cycle arrest, loss-of-function mutations to p53 can result in DNA damage tolerance at the expense of genomic fidelity. A loss of p53 in cancer allows cancerous cells to evade the induction of apoptosis as a consequence of DNA-damage because p53 is required for signaling pathways to sense DNA damage and fully respond by arresting the cell. As a result, p53-null cancers exhibit resistance to DNA-damaging chemotherapeutic agents and are unable to activate programmed cell death via p53. To broadly treat p53-null cancers in a manner that is safe

for patients (or, cancer-specific), alternative apoptotic agents encoded in the genomes of viruses may be a viable route to the development of new therapeutics.

Circoviridae are small, non-enveloped viruses with a 1.8-2.1 kb single strand DNA genome that are packaged in icosahedral virions [14]. These viruses are known to infect mammalian species including birds, pigs, bats, and humans. The most studied of these viruses is the chicken anemia virus (CAV) for two reasons. First, CAV is responsible for the death of chickens and consequently, has a severely negative impact on farming. Second, CAV contains a protein in its third ORF that is known to strongly and selectively induce apoptosis during G2/M phase in transformed cells while leaving healthy cells intact [15]. Additionally, the selective apoptotic activity of CAV-VP3, otherwise known as apoptin, is p53-independent and is marked by a cell type-specific localization to the cytoplasm of primary cells and to the nucleus of transformed cells [15]. Apoptin is a 121-residue protein which contains a nuclear export sequence (NES) from residues 37 to 46 and a lysine- and arginine-rich bipartite nuclear localization sequence (NLS) from residues 86-88 and 116-118 [15]. Both the NES and bipartite NLS are known to be required for apoptin's nucleocytoplasmic shuttling behavior, and the region of the protein containing the NLS contributes to interactions with the Anaphase Promoting Complex subunit 1 (APC1) [16]. Ultimately, both of these regions of apoptin work in tandem to produce a cell type-specific localization which further allows the protein to induce p53-independent apoptosis via nuclear localization and interaction with the APC/C in transformed cells [15].

Closely related to CAV are other well studied members of the *Circoviridae* family, porcine circoviruses (PCV). Currently, two types of PCV are known: PCV1 and PCV2, which has two subtypes. Both types of PCV are endemic to pigs; however, PCV1 is nonpathogenic while PCV2 has been implicated as a causative agent for postweaning multisystemic wasting syndrome in pigs [17]. Like CAV, the PCVs contain an ORF1 and ORF2 that produce viral replicase and capsid proteins as

well as an ORF3 coding for proteins with apoptotic capabilities that are p53-independent [18]. Despite being nonpathogenic, PCV1-VP3 has been shown to be a more potent inducer of apoptosis in transformed cells than its pathogenic counterparts PCV2a-VP3 and PCV2b-VP3 [18]. Additionally, PCV1-VP3 contains an extended C-terminal region (105-206), otherwise called “Tail,” that exhibits apoptotic capability independent of the “Core” region (1-104) and may harbor residues recognized for nuclear export [19, 20, 21] PCV1-VP3 also contains a hydrophobic region stretching from residues 105-139 that is predicted to be a transmembrane α -helix by secondary structure prediction models such as Phyre 2 and PSIPRED when coupled with the MEMSAT-SVM transmembrane fragment prediction method [34, 35, 36, 37]. Features of PCV1-VP3 and hypothesized functional regions are summarized in Figure 1. Unlike apoptin, PCV1-VP3 does not exhibit cell type-specific localization and localizes to the cytoplasm in both primary cells and transformed cells [22]. Despite the differences in localization behavior, PCV1-VP3 still retains the ability to induce apoptosis during G1/S in cells lacking a functional p53 gene while also maintaining apoptotic specificity for transformed cells [22]. The ability of PCV1-VP3 to induce a phenotypic response that is seemingly identical to apoptin implies that the steady state localization of apoptin may not be a necessary element for apoptosis induction with cell type specificity. As a result, characterizing the functions and pathways of PCV1-VP3 is of key interest for drug development because delivery of a cytoplasmic anti-cancer agent would prove less difficult to engineer than a nuclear agent.

The unique nucleocytoplasmic shuttling of apoptin has been shown to be mediated by the Chromosomal Maintenance I pathway (CRM1) [15]. CRM1 pathway protein, Exportin-I, is the primary mammalian export protein responsible for shuttling macromolecules and RNAs across the nucleus and cytoplasm [23]. Proteins that are shuttled via the CRM1 pathway contain nuclear export sequences (NES)—conserved and leucine-rich sequences generally located near the N-terminus [24]. As PCV1-VP3 shares sequence homology clustered around identified nuclear import

and export sequences of apoptin, it has been hypothesized that PCV1-VP3 and apoptin would have similar CRM1 dependent shuttling functionalities [22]. NetNES predictive software was used to predict the presence and the location of nuclear export sequences within PCV1-VP3. NESs that adhere to the canonical sequence (L-(2,3)-[LIVFM]-(2,3)-L-X-[LI]) were predicted to be located at residues 42-49 (NES1) and 134-149 (NES2) [22]. Additionally, residues 127-136 (NES3) were predicted to contain a putative NES after overlaying known export sequences of apoptin with predictions for PCV1-VP3 from the NESbase [22]. These three predicted NESs were mutated; however, PCV1-VP3 still localized in the cytoplasm [20]. Due to the ineffective knockout and elusive nature of the three NESs in conjunction with the structural predictions, it is possible that PCV1-VP3 functions via a CRM1 independent mechanism.

As a cancer-killing agent, it is likely that PCV1-VP3 engages in specific protein-protein interactions in order to “sense” the difference between a cancer cell and a primary cell, and to induce a cell cycle arrest followed by apoptosis. Apoptin induces a G2/M arrest in cancer cells before induction of apoptosis, while PCV1-VP3 has been found to induce a G1 arrest [16,22]. Past efforts to investigate binding interactions of apoptin revealed that it interacts with the anaphase promoting complex subunit cdc27; however, the molecular and conformational mechanisms of this interaction, as well as its functional consequences, remain unknown [16]. Initial research into cdc27 binding by PCV1-VP3 indicated that an interaction may occur, but the findings require further investigation due to the discovery of independent functions for PCV1-VP3 Core and Tail [19,25]. The precedent for functionally independent regions in PCV1-VP3 now demands that cdc27-binding be studied not only for the full-length protein, but for the Core and Tail regions individually, as well.

Characterization of the functional capabilities of the Core and Tail may provide insight regarding the homology between PCV1-VP3 and Apoptin, and may reveal a critical part of these proteins’ mechanisms of cancer-killing. Identification of PCV1-VP3’s binding targets and their respective binding sites is a necessary step towards developing a small-molecule drug against p53-null

cancers. Though the role of cdc27 binding with Apoptin and PCV1-VP3 is currently undefined, it could prove to be a critical part of these proteins' cancer sensitivity or their killing mechanisms.

Methodology

Transformation of JM109 Competent *E. coli*

E. coli stocks (50 μ L) were removed from storage at -80 °C and were thawed on ice. Once thawed, 5 μ L of DNA plasmid was added to cells and mixed. The cells were incubated on ice for 15-20 minutes before being heat shocked at 42 °C for 60 seconds. The cells were then incubated on ice for 2 minutes before being recovered in 450 μ L of warm Super Optimal Broth (SOB medium) and incubated at 37°C in an orbital shaker for approximately 1 hour. After recovery, 250 μ L of cell suspension was added to a flask containing 50 mL of Luria Broth (LB) with 1X antibiotics. The flasks were incubated for 18-24 hours at 37 °C in an orbital shaker.

Medium Scale Plasmid Purification

DNA plasmids were purified as outlined in the PureYield Plasmid Midiprep System #TM253. Inoculated flasks which were incubated overnight at 37 °C in the orbital shaker were removed and 50 mL of their contents were transferred to conical tubes. The cells were pelleted at 5,000 rcf for 10 minutes. The supernatant was discarded and the pellet was re-suspended in 3 mL of Resuspension Solution. Cell Lysis (3 mL) was added and the tubes were inverted 5 times; the tubes were incubated at room temperature for 3-5 minutes before Neutralization Solution (5 mL) was added after which tubes were inverted 10 times. The lysate was centrifuged at 15,000 rcf for 15 minutes. Clearing columns were inserted into binding columns. The column assembly was inserted into conical tubes. The supernatant was transferred to the clearing columns and centrifuged at 2750 rpm for 5 minutes in a swinging rotor bucket. The supernatant and clearing columns were discarded. Endotoxin Removal Wash (5 mL) was centrifuged through the binding column, followed

by 20 mL of Column Wash solution at 2750 rpm for 5 minutes each. The supernatant was discarded and the column membranes were subjected to a dry spin of 1 minute at 2750 rpm. The binding columns were placed into new 50 mL conical tubes. Warmed TE buffer (600 μ L) was added to the membrane and the assembly was centrifuged at 2750 rpm for 5 minutes. The concentration of the eluted plasmid was determined by a NanoDrop Lite Spectrophotometer (Thermo Scientific) and subsequently transferred to and stored in an Eppendorf tube at -20°C.

Cell Culture Maintenance

Non-small cell lung carcinoma cells (H1299) were maintained using Dulbecco's Modified Eagle Medium containing 10% Fetal Bovine Serum and 1% Penicillin/Streptomycin/Fungicide (D10 Medium). Cells were passed when they were 80-90% confluent in order to maintain optimal growth conditions. To pass the cells, old D10 medium was aspirated off the cells. Cells were washed with 1X Phosphate Buffered Saline (PBS) before being treated with 0.25% trypsin. The trypsin was curtailed over the cells for approximately 15 seconds and immediately aspirated off. Cells were re-suspended in fresh D10 medium and transferred to a 15 mL conical tube. The cells were centrifuged for 5 minutes at 1500 rpm in a swinging rotor bucket. The D10 medium was aspirated off and the pelleted cells were re-suspended in fresh D10. The cells were thoroughly re-suspended via vigorous pipetting in order to avoid cell clumping. Cell suspension was transferred to a new culture flask which contained additional fresh D10 medium. The culture flasks were incubated at 37°C and 5% CO₂ until the cells required further maintenance or were required for experiments.

Transient Transfections

H1299 Cells were passed into 6-well dishes containing glass coverslips prior to transfection and allowed to reach 80% confluency prior to transfection. For single well transfections using the Qiagen Effectene Transfection Reagent Kit, an optimized amount of plasmid DNA based on each DNA preparation was diluted to 100 μ L in Buffer EC. Enhancer (3.2 μ L) was added to the mixture,

mixed by flicking or vortex, and incubated at room temperature for 5 minutes. Effectene Reagent (10 μ L) was added to DNA-Enhancer mixture and flicked to ensure complete mixing. Tubes were incubated at room temperature for 15 minutes while old D10 Medium was aspirated from cells. Cells were washed with PBS before 1.6 mL of fresh D10 Medium was added. After incubation, D10 Medium (600 μ L) was added to DNA complexes before adding 600 μ L of the final mixture to the well. Plates were gently swirled to mix and returned to the incubator.

Inhibition of the CRM1 Pathway via N-ethylmaleimide

After incubating for approximately 24 hours at 37°C, the 6-well dishes were removed from the incubator and the old D10 Medium was aspirated off and the cells were washed with 1X PBS. Fresh D10 Medium (1.4 mL) was added to each well. The cells were treated for 60 minutes with 400 μ L of N-ethylmaleimide (NEM) to achieve the optimized final concentration 10mM. Control wells that were not treated with NEM received an additional 400 μ L of D10 Medium [Fig.2]. After 60 minutes of incubation, the reaction was quenched by aspirating off the D10 Medium and fixing the cells. Images of GFP were obtained using a Leica Point Scanning Confocal SP5 and analyzed using ImageJ. Statistical analysis of experimental groups was conducted using R-project version 3.3.3. Mean nuclear/cytoplasmic ratios were calculated for each construct and each drug treatment subgroup. Analysis of Variance (ANOVA) was used to determine significance levels in tests of differences between mean nuclear/cytoplasmic ratios of each treatment group. The Tukey test was used to generate adjusted confidence intervals to correct for potential false positives.

Cell Fixation

After N-ethylmaleimide treatment or cell cycle arrest treatment, old D10 Medium was removed from 6-well dishes and cells were washed with 1X PBS (2 mL). Cells were then fixed with 4% paraformaldehyde (1 mL) for 15 minutes on a 3D rotator. Glass coverslips were then mounted on microscopy slides using 15 μ L of mounting medium containing DAPI.

Cell Synchronization

Aphidicolin was prepared in an ethanol solution at 1 mg/mL before being added to D10 tissue culture media. H1299 cells were synchronized in G1 by adding 3 µg/mL aphidicolin to culture media for 18-24 hours. After this initial treatment, drug-containing media was aspirated and cells were washed with PBS before receiving fresh D10. A second, identical treatment of aphidicolin was applied 5-6 hours after changing media.

Time-Course Localization Assay

Synchronized cells were seeded in 6-well plates on microscopy cover glass immediately following release from aphidicolin treatment and allowed to grow for 24 hours. The cells were then transfected using Effectene Kits. After transfecting for 24 hours, batches of cells were fixed in 4% paraformaldehyde at 2-hour intervals for 12 hours. Samples were examined for GFP fluorescence using confocal and epifluorescence microscopy.

FLAG Immunoprecipitation

H1299 cells were grown in 10 cm dishes and transfected with FLAG-tagged protein constructs using Effectene Kits upon reaching 40-50% confluence. After 48 hours, cells were trypsinized and collected via centrifugation at 1000xg for 5 minutes. Cell pellets were resuspended in sterile PBS to wash, and pelleted again. The supernatant was removed, and cell pellets were resuspended in 500 µL ice-cold Buffer X prepared with protease inhibitors and transferred to 1.5 mL Eppendorf tubes to lyse for 20 minutes on ice. Lysates were pelleted at 1000xg for 1 hour; afterwards, the supernatant was transferred to a new tube. To each tube of cellular extracts, 10 µL of EZview Red ANTI-FLAG M2 beads were added. Tubes were incubated with EZview beads for 2-4 hours, or overnight, at 4°C. After immunoprecipitation, tubes were centrifuged at 1000xg for 1 minute to pellet the EZview beads, and samples were then resuspended in 500 µL of Buffer X to wash the samples. This wash procedure was repeated 5 times, and samples were resuspended in 50 µL of 5X

Protein Loading Buffer after the final spin and stored at 4°C. Samples were boiled at 95°C either immediately prior to storage or prior to loading for SDS-PAGE.

SDS-PAGE

A 12% resolving gel was prepared in a 15 mL conical tube by combining 3.4 mL ddH₂O, 4.0 mL 30% Bis/Acrylamide (1:19), 2.5 mL 4X resolving gel buffer (1.5M Tris-HCL, pH 8.8), and 0.1 mL 10% w/v SDS. To this solution, 50 µL 10% w/v ammonium persulfate (APS) and 7 µL tetramethylethylenediamine (TEMED) were added to catalyze gel polymerization. The final solution was poured into the gel assembly until it reached 1-2 cm from the top. Approximately 1 mL of isopropanol was gently placed on top to prevent oxygen gas from inhibiting polymerization. The stacking gel was then prepared in a 15 mL conical tube by combining 3.05 mL ddH₂O, 0.65 mL 30% Bis/Acrylamide (1:19), 1.25 mL 4X stacking gel buffer (0.5 Tris-HCL, pH 6.8), and 0.05 mL 10% w/v SDS. Once the resolving layer had fully polymerized, the isopropanol was decanted out of the gel assembly. Gel polymerizing agents, 25 µL 10% APS and 5 µL TEMED, were added to the stacking gel to begin catalysis. The stacking gel was poured on top of the resolving layer, and a comb was inserted to establish wells. The stacking gel was allowed to polymerize prior to transfer into the running cassette for electrophoresis. The assembled running cassette was immersed in running buffer (25mM Tris, 20mM glycine, pH 8.3 with 1.0% SDS). The samples were loaded into the wells and electric current was applied to produce a constant 20 mA until the bromophenol indicator of the loading buffer ran off the end of the gel.

Western Blots

A transfer assembly was constructed such that the electric field would draw the protein from the gel to PVDF (Immobilon-P) membrane. Before assembly, the PVDF membrane was equilibrated in 100% methanol for 1-2 minutes. The transfer assembly was submerged in transfer buffer and the

entire transfer dock was surrounded by ice. Constant 200 mA current was applied for one hour. The membrane was removed from the assembly and the bounds of the SDS-PAGE gel were notated on the membrane with a #2 graphite pencil. To check the transfer efficiency, the membrane was rinsed with ddH₂O before being stained with Ponceau S. (0.1% w/v in 5% acetic acid) for 1 minute. Membrane was placed in blocking buffer with shaking for 1 hour (note: blocking can be done at 4°C overnight). The membrane was washed in TBS-T for 5 minutes with shaking five times. The primary antibody was diluted 1:5000 in blocking buffer and added to the blot for an incubation period of 1 hour. The membrane was again washed in TBS-T for 5 minutes with shaking five times. The secondary antibody was diluted 1:5000 in blocking buffer and added to the blot for an incubation period of 1 hour. The blot was washed again in TBS-T for 5 minutes with shaking five times, and then in TBS for 5 minutes with shaking two times.

One method used to develop the western was with a goat anti-mouse Ig secondary antibody conjugated to alkaline phosphatase (AP). AP substrate (BCIP/NBT tablet) was dissolved in 10 mL of ddH₂O and added to the membrane. The membrane was incubated until blue-purple bands were clearly visible and was then imaged with the BioRad Chemidoc. The other development method involved the use of a mouse Anti-FLAG antibody conjugated to horseradish peroxidase (HRP). Development of the blot was conducted with Pierce ECL Western Blotting Substrate. A pre-mix of the two ECL reagents (1:1) was prepared and was added to the blot in a drop wise fashion. The blot was then imaged with the BioRad Chemidoc using the ChemiHigh Resolution setting in Image lab software set to a long exposure (5-20 seconds).

Results

Approximately 50% of cancer types contain loss of function mutations to the tumor suppressor gene p53; thus, there is an obvious need for cancer therapies that can operate independently of the

p53 pathway [source 7 from intro]. Interestingly, a subset of viruses from the *Circoviridae* family produce proteins that have been shown to selectively induce apoptosis in transformed cells in a p53 independent manner while leaving healthy cells intact [18, 26, 27, 28]. Two of these circoviruses, chicken anemia virus and porcine circovirus type 1, have been investigated intensely in regard to whether the apoptotic capabilities of each viral protein necessitate subcellular localization specificity. It has been observed that CAV-VP3 is a nucleocytoplasmic shuttling protein that is CRM1 dependent. Due to their homology and the heavily cytoplasmic localization of PCV1-VP3, it was hypothesized that PCV1-VP3 has a strong nuclear export sequence. Previous attempts to disrupt localization have included targeted mutagenesis to leucine-rich and highly hydrophobic regions of the protein that show significant sequence homology with established nuclear export sequences of the CRM1 pathway [20,30]. The subcellular localization of these various mutants was observed to have been unaltered, which indicates that alternative strategies are required to elucidate the nuclear export mechanism of PCV1-VP3.

Exhaustive mutation of regions of PCV1-VP3 that contained canonical CRM1 NES-like regions did not reveal further information regarding the protein's localization mechanism. Thus, to determine the role of CRM1 in the localization of PCV1-VP3, an assay was developed and conducted to inhibit the CRM1 nuclear export protein (Exportin 1) and analyze the subcellular localization of PCV1-VP3. A similar assay using Leptomycin B had been used to determine that CAV-VP3 was CRM1-dependent [15]; however, Leptomycin B is extremely labile, and consequently, could either introduce unwanted variability to the assay or not work as an inhibitor at all. Past studies of CRM1-dependent nuclear export demonstrated N-ethylmaleimide (NEM) to be an effective *in vivo* inhibitor of CRM1 [30, 31, 32]. To confirm the effectiveness of NEM as a CRM1 inhibitor, a protein that would exhibit both CRM1-dependent export and cytoplasmic localization was required as a positive control. Thus, an Apoptin construct with a mutated nuclear localization sequence (Ap-pmNLS) was used because it exhibits CRM1-dependent nuclear export, but accumulates in the

cytoplasm of transformed cells due to the disruption of its bipartite NLS [15]. Inhibiting CRM1 in H1299 cells transfected with GFP-tagged Ap-pmNLS is expected to result in protein accumulation in the nucleus, rather than in the cytoplasm.

PCV1-VP3 Exhibits CRM1-Independent Subcellular Localization

To determine if PCV1-VP3 wt and its subdomains are CRM1-dependent, an assay featuring NEM as a chemical inhibitor of the CRM1 pathway was designed [Fig. 2]. Once the cells reached 80% confluency, PCV1-VP3 wt (1-207aa), VP3 Core (1-105aa), VP3 Tail (105-207aa), and Ap-pmNLS constructs in eGFP-C vectors were transfected into H1299 cells; the cells were then incubated for 24 hours. After incubation, the cells were treated with a final concentration of 10mM NEM for 1 hour in order to inhibit CRM1 activity, while control groups received no drug treatment in order to provide data on the normal localization pattern of each construct. Fixed cells were mounted in a DAPI containing media and were subsequently imaged using a Leica Point Scanning Confocal SP5 microscope. Image analysis was conducted using ImageJ software. The subcellular localization of GFP-tagged proteins was quantitatively assessed by measuring the ratios of nuclear and cytoplasmic GFP intensity in individual cells. Cells expressing eGFP were used to normalize nuclear/cytoplasmic ratios of the experimental groups by setting the localization pattern of eGFP as the baseline for equal signal intensity in both regions. GFP-tagged Ap-pmNLS exhibited a statistically significant shift in subcellular localization from the nucleus to the cytoplasm when cells were treated with NEM. PCV1-VP3 wt, Core, and Tail all exhibited no significant subcellular localization shift when CRM1 was inhibited. The localization patterns of each construct under control and drug-treatment conditions were confirmed in three independently executed experiments. Wild-type PCV1-VP3 and the Tail subdomain (105-207) exhibit predominately cytoplasmic localization patterns that are independent of the state of CRM1 activity, while PCV1-VP3's Core subdomain (1-105) remains predominately nuclear regardless of CRM1 activity [Fig. 3]. This assay ultimately demonstrated that PCV1-VP3 wt and its subdomains exhibit CRM1-

independent subcellular localization, and that the Core and Tail subdomains exhibit unique patterns of localization when separated.

Time Course Assay of PCV1-VP3 Subcellular Localization

In large populations of cells ($n > 300$), roughly 10% of cells transfected with PCV1-VP3 wt do not follow the representative pattern of subcellular localization. In these cells, PCV1-VP3 appears to accumulate in the nucleus. This observation, in conjunction with new findings showing that PCV1-VP3 localization is not CRM1-dependent, prompted an investigation of PCV1-VP3 subcellular localization throughout the cell cycle in H1299 cells in order to determine if its localization is a cell cycle-dependent effect. Cultures of H1299 cells were arrested in early S phase using aphidicolin, a reversible inhibitor of DNA polymerase alpha, and were subsequently transfected with GFP-tagged wild-type PCV1-VP3. Cells were fixed at 2-hour intervals in order to capture cell cycle progression from S phase to the following G1 phase. Preliminary results revealed uniformly atypical patterns of wild-type PCV1-VP3 localization that fail to recapitulate canonically observed localization patterns. While the localization pattern was not precisely what is normally observed for PCV1-VP3 wt, there was no apparent cell cycle-dependency for the localization patterns of PCV-VP3 wt [Fig. 4].

Western Blotting of FLAG and cdc27

Apoptin was previously shown to interact with the Anaphase Promoting Complex subunit cdc27 (APC3) by western blot [16]. Cdc27 interactions are of key interest because of the crucial role that the APC/C plays in cell cycle arrests, another hallmark of apoptin and PCV1-VP3 activity in cancers. Given the homology between apoptin and PCV1-VP3, western blots were used to assess cdc27 interactions for PCV1-VP3 wild type as well as the Core and Tail subdomains. Prior research indicated that PCV1-VP3 will co-immunoprecipitate with cdc27, but results proved largely inconclusive and warranted further investigation. H1299 cells were transfected with FLAG-tagged proteins of interest and were harvested for protein purification by immunoprecipitation (IP). A

western blot against the FLAG tag carried out with samples separated by SDS-PAGE revealed that only the FLAG-apoptin construct was successfully expressed in H1299 cells and isolated by the IP [Fig. 5A]. Furthermore, western blots against *cdc27* confirmed past findings that apoptin pulls down *cdc27* in a co-IP [Fig. 5B]. No bands at the expected size of *cdc27* were visible in lanes containing immunoprecipitation samples from cells transfected with PCV-VP3 constructs.

Discussion

Subcellular localization of PCV1-VP3 is under intense scrutiny as a prerequisite for the induction of apoptosis. Here, an assay to determine the dependency of PCV1-VP3 on CRM1 for nuclear export was conducted. Experimental results indicated that export of PCV1-VP3 is not a CRM1-dependent process [Fig. 3]. Furthermore, the two subdomains of PCV1-VP3, Core and Tail, displayed nuclear and cytoplasmic localization respectively in a CRM1-independent manner [Fig. 3]. There are three distinct possibilities that explain the localization pattern of PCV1-VP3: nucleocytoplasmic shuttling via an alternative export mechanism, sequestering of the protein in the cytoplasm, or synthesis of PCV1-VP3 which localizes in a diffuse manner throughout the cytoplasm. To determine which possibility was most likely, a time course assay of a synchronized cell population was conducted in order to monitor the movement of PCV1-VP3 throughout the cell cycle. If PCV1-VP3 undergoes dynamic nucleocytoplasmic shuttling via an alternative mechanism, the protein's movement throughout the cell would be reflected in fluctuations of its concentration in cellular compartments. In contrast, if PCV1-VP3 is cytoplasmic and does not undergo dynamic shuttling, its localization pattern will remain cytoplasmic until the nuclear envelope breaks down in preparation for cell division; at this point, PCV1-VP3 will diffuse throughout the entirety of the cell. If sequestered, PCV1-VP3 localization will not change even in the absence of a nuclear envelope.

Preliminary results revealed problems with both cell health and GFP expression levels after treatment with aphidicolin [Fig. 4]. The uniformly localized GFP signal throughout cell and intense

nucleolar signal suggests overexpression of protein due to either an error in transfection or a by-product of the aphidicolin treatment that is not documented in the literature. Multiple attempts to repeat this assay were made; however, cell viability decreased drastically after seeding and transfection events. As a result, there was an insufficient population of viable cells available to conduct the experiment. Due to insufficient time and resources, the exact features of the assay that were leading to decreased viability were not pinpointed. However, it is possible that cell passage immediately following a double arrest with aphidicolin exerts excessive stress and leads to cell detachment and death; thus, future researchers attempting to optimize this assay should seed unsynchronized H1299s in 6-wells and conduct chemical synchronization directly in the wells. Additionally, further troubleshooting is required to determine optimal methods for handling synchronized H1299 cells due to the observed issues with transfection and GFP overexpression.

Whether PCV1-VP3 is sequestered in the cytoplasm or exported via an alternative mechanism, the findings of the NEM assay point to an unexpected mechanistic divergence between PCV1-VP3 and its homolog, Apoptin. To explore the degree of diversity further, Immunoprecipitation and Western blots with Anti-cdc27 primary antibody were conducted. Cdc27 was successfully pulled down with Apoptin by immunoprecipitation; however, PCV1-VP3 wild type, Core, and Tail all exhibited no observable interaction with cdc27 [Fig. 5B]. This result failed to confirm past research that found PCV1-VP3 to be capable of interacting with cdc27. However, this result does not necessarily point to a reversal of previous findings of PCV1-VP3 co-precipitation with cdc27 but rather suggests that there is inadequate expression of FLAG-tagged PCV1-VP3 constructs given that the blot probed with Anti-FLAG antibody did not produce a band for any of the PCV1-VP3 constructs [Fig. 5A]. Future researchers should dedicate more time to confirm adequate expression of FLAG-tagged PCV1-VP3 constructs before attempting to confirm PCV1-VP3 interactions with and the functional capabilities of Core and Tail with respect to cdc27 interactions.

The functions of Core and Tail are of critical interest because previous research found the Tail to be independently capable of inducing apoptosis, and NEM studies revealed that Core and Tail can localize to the nucleus and cytoplasm, respectively, in an independent manner. The subdomains clearly exhibit unique functions, but the degree to which each subdomain directs localization, cancer sensitivity, and apoptosis induction by full-length PCV1-VP3 are still unknown. It is possible that the Tail region alone is sufficient for cancer-specific apoptosis, but this must be confirmed by cell death assays in H1299 cells and primary cells. The possibility still exists that the Tail subdomain is simply a toxic protein and causes indiscriminate cell death. In that case, Tail would therefore be a poor drug-design candidate because it would lack cancer specificity. Furthermore, the search for anti-cancer drug targets demands investigation of the PCV1-VP3 interactome. PCV1-VP3 may have critical cancer-sensing mechanisms that are unrelated to cdc27 interactions. Past investigations of apoptin used immunoprecipitation coupled with mass spectrometry to analyze potential protein-protein interactions worthy of further study, and the same could be done for PCV1-VP3. In any future studies of PCV1-VP3 functions, both cancer cells and primary cells should be assayed in order to screen for cell type-specific effects. Any feature of PCV1-VP3 that demonstrates cancer specificity may be a turning point in the search for a drug target.

Figures & Tables

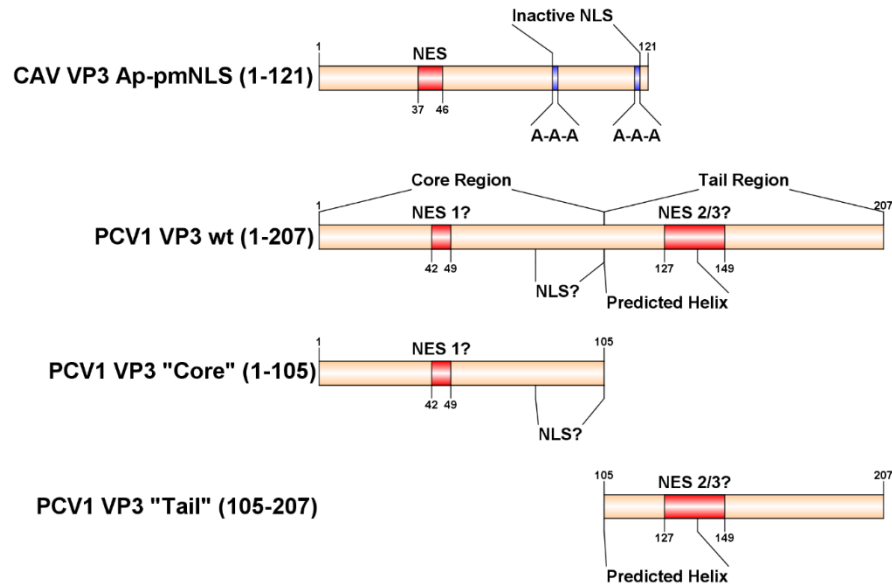


Figure 1. Protein feature map of proteins used for transfection experiments.

Number markings denote amino acid residues corresponding to the length of each protein as well as the positions of known functional regions within each protein. For PCV1 VP3 wt (wild-type), NES locations previously predicted by NetNES and NESbase are also shown. Protein map was produced using IBS 1.0.1 *Illustrator for Biological Sequences* (Liu 2015, *Bioinformatics*) [33].

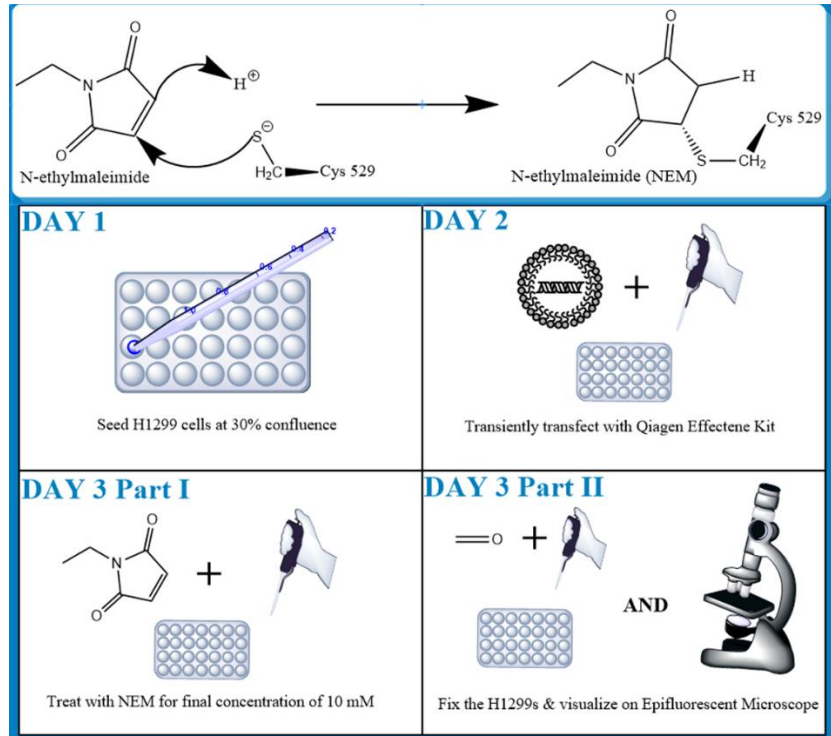


Figure 2. Workflow for NEM CRM1 inhibition assay.

H1299 cells were seeded in 6-well dishes at 30% confluence. After a 24 hr. incubation, the cells were transiently transfected (70-80% confluency) and were incubated for an additional 24 hrs. The cells were treated with NEM (final concentration 10mM) for 60 mins and were subsequently fixed with paraformaldehyde, DAPI stained, and mounted.

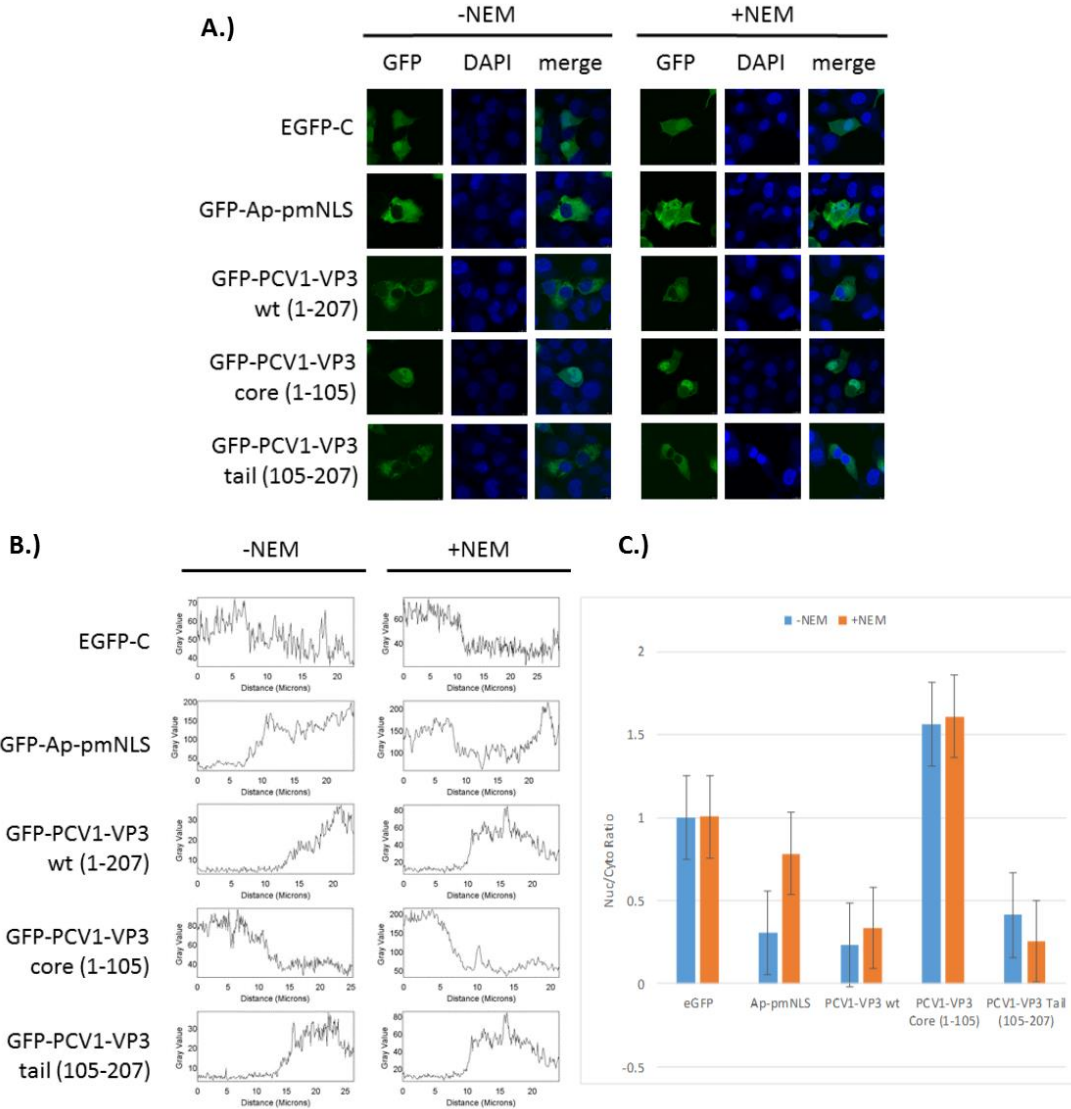


Figure 3. (A) N-ethylmaleimide Assay Confocal imaging.

Leica Point Scanning Confocal SP5 images of control and NEM-treated H1299 cells transfected with GFP-fusions to Aoptin and PCV1 VP3 mutants. For each construct row, -NEM denotes untreated cells and +NEM denoted cells treated with 10mM N-ethylmaleimide CRM1 inhibitor prior to fixation. For each construct row, -NEM denotes untreated cells and +NEM denoted cells treated with 10mM N-ethylmaleimide CRM1 inhibitor prior to fixation. GFP and DAPI channels were captured sequentially to minimize DAPI-to-GFP bleed-through. Images from the 40x objective were captured in 1024x1024 resolution at 100Hz scan speed. **(B.)** ImageJ was used to generate pixel intensity graphs of lines drawn from the inner wall of the nucleus to the cytoplasm.

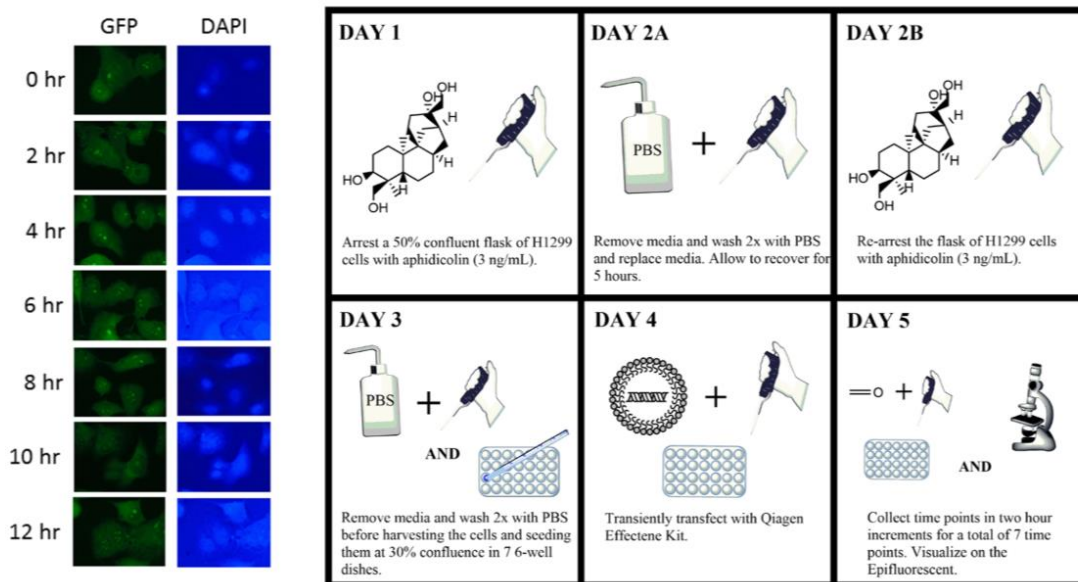


Figure 4. Time Course Imaging of PCV1-VP3 wild type; aphidicolin arrest protocol.

H1299 cells were arrested twice in early S phase for 24 hours using aphidicolin. Synchronized cells were seeded in 6-well dishes on cover slides and transfected with GFP-tagged PCV1-VP3 constructs 24 hours after seeding. Cells were fixed over 12 hours at 2 hour intervals and imaged using a Zeiss Vert A.1 epifluorescence microscope. The localization of wild type PCV1-VP3 failed at all observed time points to recapitulate the pattern shown in the NEM assay control [Fig. 3A], which indicated that further optimization of GFP tag expression and aphidicolin arrest may be required before any observation can be made regarding the cell cycle-dependency of PCV1-VP3 localization.

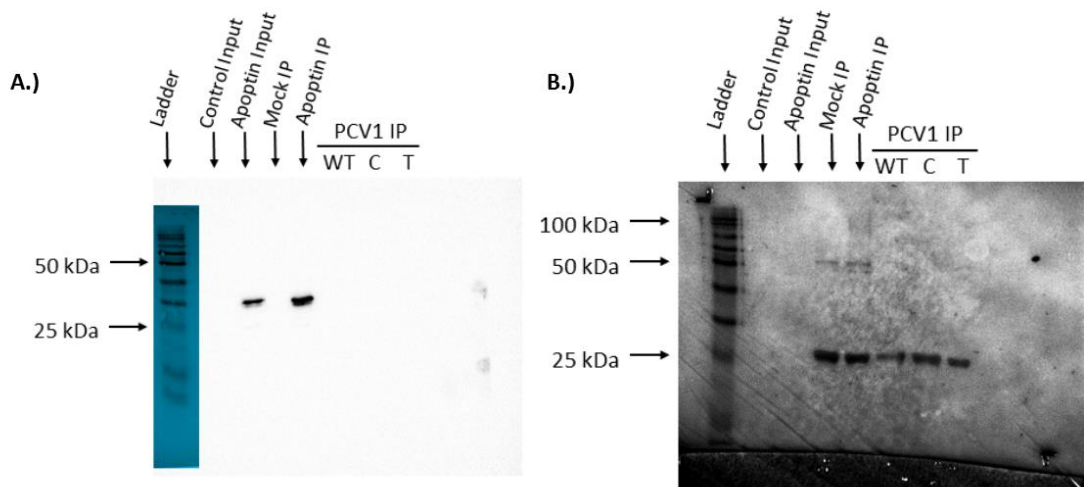


Figure 5. Western Blotting for FLAG and cdc27.

Each cell extract sample was split before Immunoprecipitation in order to provide Input controls for western blotting. "Control Input" represents cell lysates from untransfected cells, while "Aoptin Input" represents cell lysates from cells transfected with FLAG-apoptin. Mock immunoprecipitation was carried out on Control Input samples and run in the lane labeled "Mock IP". **(A.)** Western blot using HRP-conjugated mouse anti-FLAG antibody. Expected FLAG bands were visible in samples from cells transfected with FLAG-apoptin, but not PCV1-VP3 or its subdomains. **(B.)** Western Blot using HRP-conjugated goat anti-mouse antibody against mouse anti-cdc27 (APC3). A band at roughly the expected size of cdc27 was observed in the immunoprecipitated FLAG-apoptin sample, but not in PCV1-VP3 or its subdomains. Western blotting confirmed prior knowledge that cdc27 associates with Aoptin in H1299 cells. The lack of observed FLAG-tagged protein in the PCV1-VP3 samples was revealed by the FLAG blot, so no determination regarding cdc27 interaction can be made.

References

- [1] Siegel, R. L., Miller, K. D., & Jemal, A. (2016). Cancer statistics, 2016. *CA Cancer J Clin*, 66(1), 7-30. doi:10.3322/caac.21332
- [2] U.S. Cancer Statistics Working Group. *United States Cancer Statistics: 1999–2013 Incidence and Mortality Web-based Report*. Atlanta: U.S. Department of Health and Human Services, Centers for Disease Control and Prevention and National Cancer Institute; 2016. Available at: www.cdc.gov/uscs.
- [3] "Cancer Statistics." National Cancer Institute. National Institutes of Health, n.d. Web. 05 Oct. 2015.
- [4] Vander Heiden, M. G., Cantley, L. C., & Thompson, C. B. (2009). Understanding the Warburg effect: the metabolic requirements of cell proliferation. *Science*, 324(5930), 1029-1033. doi:10.1126/science.1160809
- [5] Cheung-Ong, K., Giaever, G., & Nislow, C. (2013). DNA-damaging agents in cancer chemotherapy: serendipity and chemical biology. *Chem Biol*, 20(5), 648-659. doi:10.1016/j.chembiol.2013.04.007
- [6] Peters, J. M. (2006). The anaphase promoting complex/cyclosome: a machine designed to destroy. *Nat Rev Mol Cell Biol*, 7(9), 644-656. doi:10.1038/nrm1988
- [7] Schafer, K. A. (1998). The cell cycle: a review. *Vet Pathol*, 35(6), 461-478. doi:10.1177/030098589803500601
- [8] Taylor, W. R., & Stark, G. R. (2001). Regulation of the G2/M transition by p53. *Oncogene*, 20(15), 1803-1815. doi:10.1038/sj.onc.1204252
- [9] Peters, J. M. (2002). The anaphase-promoting complex: proteolysis in mitosis and beyond. *Mol Cell*, 9(5), 931-943.
- [10] Kubbutat, M. H., Jones, S. N., & Vousden, K. H. (1997). Regulation of p53 stability by Mdm2. *Nature*, 387(6630), 299-303. doi:10.1038/387299a0
- [11] Shieh, S. Y., Ikeda, M., Taya, Y., & Prives, C. (1997). DNA damage-induced phosphorylation of p53 alleviates inhibition by MDM2. *Cell*, 91(3), 325-334.
- [12] Chuikov, S., Kurash, J. K., Wilson, J. R., Xiao, B., Justin, N., Ivanov, G. S., . . . Reinberg, D. (2004). Regulation of p53 activity through lysine methylation. *Nature*, 432(7015), 353-360. doi:http://www.nature.com/nature/journal/v432/n7015/supinfo/nature03117_S1.html
- [13] Brown, J. P., Wei, W., & Sedivy, J. M. (1997). Bypass of Senescence After Disruption of p21^{CIP1/WAF1} Gene in Normal Diploid Human Fibroblasts. *Science*, 277(5327), 831-834. doi:10.1126/science.277.5327.831
- [14] Rosario, K., Breitbart, M., Harrach, B., Segalés, J., Delwart, E., Biagini, P., & Varsani, A. (2017). Revisiting the taxonomy of the family Circoviridae: establishment of the genus Cyclovirus and removal of the genus Gyrovirus. *Archives of Virology*, 162(5), 1447-1463. doi:10.1007/s00705-017-3247-y

- [15] Heilman, D. W., Teodoro, J. G., & Green, M. R. (2006). Apoptin Nucleocytoplasmic Shuttling Is Required for Cell Type-Specific Localization, Apoptosis, and Recruitment of the Anaphase-Promoting Complex/Cyclosome to PML Bodies. *Journal of Virology*, *80*(15), 7535-7545. doi:10.1128/JVI.02741-05
- [16] Teodoro, J. G., Heilman, D. W., Parker, A. E., & Green, M. R. (2004). The viral protein Apoptin associates with the anaphase-promoting complex to induce G2/M arrest and apoptosis in the absence of p53. *Genes Dev*, *18*(16), 1952-1957. doi:10.1101/gad.1198404
- [17] Cortey, M., & Segalés, J. (2012). Low levels of diversity among genomes of Porcine circovirus type 1 (PCV1) points to differential adaptive selection between Porcine circoviruses. *Virology*, *422*(2), 161-164. doi:http://doi.org/10.1016/j.virol.2011.10.014
- [18] Chaiyakul, M., Hsu, K., Dardari, R., Marshall, F., & Czub, M. (2010). Cytotoxicity of ORF3 Proteins from a Nonpathogenic and a Pathogenic Porcine Circovirus. *Journal of Virology*, *84*(21), 11440-11447. doi:10.1128/jvi.01030-10
- [19] Filatava, E. J., Vu, P. T. (2015). Truncation mutagenesis of Porcine Circovirus 1 VP3 uncovers the importance of the C-terminal extended region in inducing apoptosis of human cancer cells: *WPI Project Reports*.
- [20] Amato, K. (2016). Apoptotic Capabilities of Porcine Circovirus 1 Viral Protein 3 as a Function of Subcellular Localization: *WPI Project Reports*.
- [21] Eisenberg, S., Hermsdorf-Krasin, L., Innamorati, C. (2013). Three-Dimensional Modeling of Chicken Anemia Virus VP3 and Porcine Circovirus Type 1 VP3: *WPI Project Reports*.
- [22] Hough, K. P., Rogers, A. M., Zelic, M., Paris, M., & Heilman, D. W. (2015). Transformed cell-specific induction of apoptosis by porcine circovirus type 1 viral protein 3. *Journal of General Virology*, *96*(2), 351-359. doi:doi:10.1099/vir.0.070284-0
- [23] Nguyen, K. T., Holloway, M. P., & Altura, R. A. (2012). The CRM1 nuclear export protein in normal development and disease. *Int J Biochem Mol Biol*, *3*(2), 137-151.
- [24] Mathur, A., Roy, T. (2015) Investigation of PCV1-VP3 Nuclear Export Signal Sequences Using Site-Directed Mutagenesis: *WPI Project Reports*.
- [25] Partlow, E. A. (2015) Apoptin and PCV1-VP3 Selectively Induce Apoptosis in Transformed Cells via a Conserved Mechanism Mediated by the Anaphase Promoting Complex: *WPI Project Reports*.
- [26] Noteborn, M. H., Todd, D., Verschueren, C. A., de Gauw, H. W., Curran, W. L., Veldkamp, S., . . . Koch, G. (1994). A single chicken anemia virus protein induces apoptosis. *J Virol*, *68*(1), 346-351.
- [27] Zhuang, S. M., Shvarts, A., van Ormondt, H., Jochemsen, A. G., van der Eb, A. J., & Noteborn, M. H. (1995). Apoptin, a protein derived from chicken anemia virus, induces p53-independent apoptosis in human osteosarcoma cells. *Cancer Res*, *55*(3), 486-489.
- [28] Oorschot, A. A. A. M. D.-V., Fischer, D. F., Grimbergen, J. M., Klein, B., Zhuang, S. M., Falkenburg, J. H. F., . . . Noteborn, M. H. M. (1997). Apoptin induces apoptosis in human transformed and

malignant cells but not in normal cells. *Proceedings of the National Academy of Sciences of the United States of America*, 94(11), 5843-5847.

- [29] Pakatar, N. (2015). Localization Assessment of Novel Nuclear Export Signal Sequence Mutants in PCV1-VP3: *WPI Project Reports*.
- [30] Kudo, N., Matsumori, N., Taoka, H., Fujiwara, D., Schreiner, E. P., Wolff, B., . . . Horinouchi, S. (1999). Leptomycin B inactivates CRM1/exportin 1 by covalent modification at a cysteine residue in the central conserved region. *Proc Natl Acad Sci U S A*, 96(16), 9112-9117.
- [31] Holaska, J. M., & Paschal, B. M. (1998). A cytosolic activity distinct from Crm1 mediates nuclear export of protein kinase inhibitor in permeabilized cells. *Proceedings of the National Academy of Sciences of the United States of America*, 95(25), 14739-14744.
- [32] Itoh, K., Brott, B. K., Bae, G.-U., Ratcliffe, M. J., & Sokol, S. Y. (2005). Nuclear localization is required for Dishevelled function in Wnt/ β -catenin signaling. *Journal of Biology*, 4(1), 3. doi:10.1186/jbiol20
- [33] Liu, W., Xie, Y., Ma, J., Luo, X., Nie, P., Zuo, Z., . . . Ren, J. (2015). IBS: an illustrator for the presentation and visualization of biological sequences. *Bioinformatics*, 31(20), 3359-3361. doi:10.1093/bioinformatics/btv362
- [34] Buchan DWA, Minneci F, Nugent TCO, Bryson K, Jones DT. (2013). Scalable web services for the PSIPRED Protein Analysis Workbench . *Nucleic Acids Research* . 41 (W1): W340-W348.
- [35] Jones DT. (1999) Protein secondary structure prediction based on position-specific scoring matrices. *J. Mol. Biol.* 292: 195-202.
- [36] Nugent, T. & Jones, D.T. (2009) Transmembrane protein topology prediction using support vector machines. *BMC Bioinformatics*. 10, 159. Epub
- [37] Kelley, L. A., Mezulis, S., Yates, C. M., Wass, M. N., & Sternberg, M. J. E. (2015). The Phyre2 web portal for protein modeling, prediction and analysis. *Nat. Protocols*, 10(6), 845-858. doi:10.1038/nprot.2015.053